Assessment of the performance of tuned range-separated hybrid density functionals in predicting accurate quasiparticle spectra

Thomas Körzdörfer, Robert M. Parrish, Noa Marom, John S. Sears, C. David Sherrill, and Jean-Luc Brédas

Phys. Rev. B **86**, 205110 — Published 8 November 2012

DOI: 10.1103/PhysRevB.86.205110

Can tuned range-separated hybrid density functionals predict accurate quasi-particle spectra?

Thomas Körzdörfer[1&], Robert M. Parrish[1], Noa Marom[2], John S. Sears[1],

C. David Sherrill[1], and Jean-Luc Brédas[1#]*

[1] Center for Organic Photonics and Electronics and Center for Computational Molecular Science and Technology

School of Chemistry and Biochemistry

Georgia Institute of Technology, Atlanta, Georgia 30332-0400

[2] Center for Computational Materials

Institute for Computational Engineering and Sciences

The University of Texas at Austin, Austin, Texas 78712-1229

* Email: jean-luc.bredas@chemistry.gatech.edu

[#] Also affiliated with Department of Chemistry, King Abdulaziz University, Jeddah 21589, Saudi Arabia

[&] New permanent address: Computational Chemistry, University of Potsdam, D-14476 Potsdam, Germany

Abstract

Long-range corrected hybrid functionals that employ a non-empirically tuned range-separation parameter have been demonstrated to yield accurate ionization potentials and fundamental gaps for a wide range of finite systems. Here, we address the question of whether this high level of accuracy is limited to the highest occupied / lowest unoccupied energy levels to which the range-separation parameter is tuned, or whether it is retained for the entire valence spectrum. We examine several π–conjugated molecules and find that orbitals of a different character and symmetry require significantly different range-separation parameters and fractions of exact exchange. This imbalanced treatment of orbitals of a different nature biases the resulting eigenvalue spectra. Thus, the existing schemes for the tuning of range-separated hybrid functionals, while providing for good agreement between the highest occupied energy level and the first ionization potential, do not achieve accuracy comparable to reliable G_0W_0 computations for the entire quasi-particle spectrum.

1. Introduction

The combination of photoelectron spectroscopy (PES) with electronic-structure calculations based on density functional theory in the Kohn-Sham (KS)[1] or Generalized Kohn-Sham (GKS)[2] framework has been used successfully to gain far-reaching physical insight, regarding, *e.g.*, the assignment of PES peaks to particular molecular orbitals, as exemplified by Refs. 3-14. It would be intriguing indeed if the complex nature of the quasi-particle (QP) spectra, which arises from intricate many-body-interactions,[15, 16] could be captured by single-particle quantities such as KS or GKS eigenvalues, in particular as the latter can be calculated from a computationally much simpler approach, *i.e.*, diagonalization of the KS or GKS Hamiltonian. In practice, interpreting KS and GKS eigenvalues obtained from semilocal or global hybrid functionals as approximations to relaxed ionization potentials (IPs) often yields good agreement with PES experiments.

Many-body perturbation theory in the *GW* approximation, where *G* represents the one-particle Green's function and *W* the dynamically screened Coulomb interaction, is currently the method of choice for calculating QP energies from first principles.[15, 16] However, due to its high computational cost, the size of the systems that can be studied with a fully self-consistent *GW* approach[17] is rather limited. Therefore, the non-self-consistent G_0W_0 approach, in which *G* and *W* are evaluated from DFT orbitals and eigenvalues, is often used. It must be borne in mind that the results of G_0W_0 calculations can depend significantly on the chosen DFT starting point.[18-22] Consequently, a DFT-based approach that could yield accurate QP energies for both occupied and unoccupied states is highly desirable, not only to extend the range of systems for which reliable QP energies can be obtained, but also as a suitable starting point for G_0W_0 calculations.

Although KS eigenvalues do not have any strict physical meaning, a close relationship between exact KS eigenvalues and QP energies exists. Following the IP-theorem,[23] the highest occupied KS eigenvalue equals the first ionization potential. All other occupied KS eigenvalues are well-defined approximations to the relaxed ionization energies to zeroth order in the adiabatic coupling constant.[5] Of course, this relation only holds for the occupied, and not the unoccupied eigenvalues. Moreover, the exact exchange-correlation (xc) functional is unknown and approximate density functionals must be employed instead. In practice, this frequently leads to severe problems with the interpretation of KS or GKS eigenvalues as approximations to QP energies, which can be summarized as follows:

(i) The eigenvalue of the highest occupied molecular orbital (HOMO) obtained from commonly used DFT functionals is typically too high in energy, *i.e.*, the predicted ionization energy is too small.

(ii) The KS eigenvalue gap between the HOMO and the lowest unoccupied molecular orbital (LUMO) is much smaller than the fundamental gap that represents the difference between the IP and electron affinity (EA), as it lacks the derivative discontinuity.[24, 25]

(iii) The KS eigenvalue spectrum typically appears to be compressed when compared to the experimental PES spectrum, *i.e.*, the level spacings are too small.

(iv) The relative ordering of eigenvalues corresponding to orbitals of a different nature (*e.g.*, localized versus delocalized or π versus σ orbitals) can be wrong, leading to severe distortions in the DFT eigenvalue spectrum.[8-12]

Recently, several publications have discussed the origin of these drawbacks.[5, 8-12, 26, 27] They ascribed points (i) and (iv) primarily to self-interaction errors (SIEs) in the employed approximate xc-functionals. Indeed, SIE-free KS-DFT[10, 11] provides for much improved

eigenvalues in terms of the HOMO and the relative ordering of the deeper-lying states. This is true not only for the orbital energies[11, 12] but also for their character,[13] even in the case of challenging systems. Calculating the so-called "orbital self-interaction error" (OSIE)[11, 12] can therefore help predict if major problems with the orbital ordering in approximate density functionals is to be expected for a given system of interest.[22] In contrast to issues (i) and (iv), issues (ii) and (iii) would persist even if the exact KS-functional was employed.[28] Consequently, they cannot be solved by improving upon existing approximations to the KS-functional. In this sense, issues (ii) and (iii) can be ascribed to effects beyond the single-particle picture, *i.e.*, many-particle effects. In the G_0W_0 approach, which is designed to include many-particle effects via many-body perturbation theory, it is the quasi-particle corrections to the KS eigenvalues that open the KS gap to equal the fundamental gap and stretch the spectrum to match the experimental PES spectrum.

The use of hybrid functionals within a GKS scheme can mimic the QP corrections by including a fraction of the exchange-only derivative discontinuity in the eigenvalues.[2, 22, 27] Overall, this leads to a stretching of the eigenvalue spectrum, an improved HOMO eigenvalue, and an increase in the HOMO-LUMO gap. In contrast to SIE-free KS approaches, the HOMO eigenvalue obtained from standard global hybrid functionals is still too small, and the relative ordering of the states may not always be correct,[13] although it is generally much improved as compared to semilocal DFT.[27] Importantly, the stretching of the eigenvalue spectrum, the relative ordering of states, the HOMO eigenvalue, and the HOMO-LUMO gap predicted from global hybrid functionals are primarily determined by the amount of HF exchange employed in the functional.[27] However, the amount of HF exchange needed to obtain an approximately correct relative occupied eigenvalue spectrum (20-25%)[22] is much smaller than that needed to correct

for the HOMO eigenvalue and the HOMO-LUMO gap (50-80%).[29] Thus, there is no global hybrid functional that yields the correct IP, fundamental gap, and quasi-particle spectrum all at the same time. In fact, both SIE-free KS and global hybrid GKS approaches have their advantages, but none of them has been demonstrated to be capable of solving all four issues related to the interpretation of KS/GKS eigenvalues as QP energies.[30]

Recently, tuned long-range corrected (LRC) hybrid functionals, in which the range-separation parameter is non-empirically tuned to satisfy exact physical constraints for the ionization potential (IP) or the fundamental gap, have been proposed as a possible solution for this problem.[31-37] The GKS eigenvalues obtained from this class of functionals can predict ionization potentials and fundamental gaps of comparable accuracy to G_0W_0 calculations at a lower computational cost,[34, 38] thus solving the two major problems of the global hybrids discussed above. Here, we analyze whether LRC hybrid functionals tuned to reproduce the IP and/or fundamental gap can retain a high level of accuracy for the entire valence spectrum in π–conjugated molecules, both in terms of the absolute energies as well as their relative ordering. It is only if the entire spectrum is predicted with sufficient accuracy, that the tuned LRC-hybrids could truly be considered as reliable, computationally low-cost alternatives to *GW* methods.

2. LRC hybrid functionals and the MSIE

The central premise underlying all LRC functionals is a separation of the Coulomb operator into short-range (SR) and long-range (LR) components, typically achieved by employing the standard error function (*erf*):

$$\frac{1}{r} = \frac{erf(\omega r)}{r} + \frac{erfc(\omega r)}{r} \quad (1)$$

The range-separation parameter, ω, determines the partitioning of the SR and LR components. Since the inception of the range-separated hybrid functionals,[39] it has been clear that ω should in fact be a functional of the density. However, the exact density dependence of ω is not known. Initially, most range-separated hybrid functionals employed a fixed value for ω, which was determined empirically.[40, 41] Later, a number of approaches have been developed that allow for a more flexible range separation. Examples include LRC hybrids with multiple ranges[42, 43] as well as the so-called "local range-separated hybrids".[44-46] Recently, an alternative strategy has been suggested,[31-36, 38] in which the single range-separation parameter is tuned separately for each system of interest. In so called "IP-tuned"[34] LRC-hybrids the optimal range-separation parameter is found by minimizing the difference between the HOMO eigenvalue and the computed IP:

$$\Delta_{IP}(\omega) = \left| -\varepsilon_{HOMO}^{\omega} - \left(E_{gs}(\omega, N) - E_{gs}(\omega, N-1) \right) \right| \quad (2)$$

The IP-tuning procedure has been shown to improve the description of properties related to the IP and the fundamental gap for a range of systems.[34, 38] The tuning is completely non-empirical, as it simply requires that the resultant generalized Kohn-Sham solution obeys a

property that would be identically satisfied for an exact Kohn-Sham or generalized Kohn-Sham approach. Other tuning procedures have been proposed to find the optimal ω, such as tuning to the fundamental gap instead of the IP[38] or tuning to minimize the many-electron self-interaction error (MSIE).[47, 48]

An approximation to the exchange-correlation (xc) functional is called free from MSIE if it captures a certain property of the exact xc functional for fractional particle numbers, *i.e.*, the total energy for fractional occupation numbers is a series of straight lines with kinks at integer occupations (piecewise linear).[49, 50] As the slope of the total energy curve is closely related to the HOMO eigenvalue via Janak's theorem,[23] the MSIE may be alternatively evaluated by the HOMO eigenvalue instead of the total energy, *i.e.*, a functional is called free from MSIE if the HOMO eigenvalue is constant for fractional occupation numbers. The IP-tuning procedure for the LRC hybrids can be interpreted as a minimization of the MSIE at the HOMO level. As the HOMO KS-eigenvalue equals the slope of the total energy, IP-tuning guarantees that the initial slope of the total energy curve at $\delta=0^-$, *i.e.*, when going from the neutral to the cation state, equals the vertical ionization potential, *i.e.*, the energy difference between neutral and cation.[32] However, this does not apply for the whole fractional particle curve, which is why a very small and typically positive MSIE remains after the IP-tuning. Still, the MSIE at the HOMO level is significantly reduced in the IP-tuned LRC-hybrids as compared to Hartree-Fock and all other commonly used semilocal, global hybrid, and standard LRC-hybrid functionals. This has recently been demonstrated by some of us for the case of polyene chains.[51]

In order to quantify the MSIE in different exchange-correlation (xc) functionals and systems of interest, we evaluate the deviation of the total energy *E* from the expected straight-line behavior:

$$\Delta E(N+\delta) = E(N+\delta) - E(N) - [E(N+1) - E(N)]\delta \qquad (3)$$

where *N* is an integer and $0 \leq \delta \leq 1$. ΔE vanishes for integer particle numbers. For fractional particle numbers however, ΔE vanishes only if $\Delta E(N+\delta)$ is linear in δ, *i.e.*, if the expression:

$$\Delta E(N+\delta) = E(N) + [E(N+1) - E(N)]\delta \qquad (4)$$

holds, as is the case for the exact xc-functional. In the following, we define the integral:

$$\int_0^1 \Delta E(N+\delta)\, d\delta \qquad (5)$$

as the orbital many-electron self-interaction error (OMSIE) corresponding to the HOMO of the N+1-electron system. Following this definition, the OMSIE can vanish although Eq. (4) does not hold, *i.e.*, a vanishing OMSIE does not necessarily imply a perfect straight-line behavior of the total energy. In contrast, a straight-line behavior of the total energy *does* imply a vanishing OMSIE. A positive OMSIE is referred to as a *localization* error, as it spuriously favors situations with integer particle numbers over situations with fractional particle numbers,[52] while a negative OMSIE is referred to as a *delocalization* error. In contrast to the original definition of the MSIE, which just qualitatively distinguishes between MSIE-free and not MSIE-free approaches, the OMSIE provides for a quantitative analysis of the MSIE in a given

approximation and system and allows distinguishing between single-particle orbitals. Although the OMSIE vanishes for the exact functional, it should be kept in mind that there is no theorem that directly relates the OMSIE to the quasi-particle energies. Consequently, a vanishing OMSIE does not guarantee an accurate quasi-particle spectrum (in particular not for deeper lying states) and vice versa.

In the present work, the range-separation parameter was tuned to the IP following Eq. (2) and the OMSIE was evaluated following Eq. (5). We note that, after this part of our work was completed and reported,[53] we became aware of a different tuning procedure to determine ω (involving the IP for the anion, neutral, and cation states) proposed by Refaely-Abramson *et al.*[48]; in addition, the authors of Ref. [48] evaluated the MSIE for the HOMO and LUMO by studying the dependence on the fractional particle number of the eigenvalues rather than the total energy (see further discussion in Section 5).

3. Computational Details

The DFT geometries for all the molecules we considered here, that is benzene, pyrimidine, 3,4,9,10-perylene-tetracarboxylic-dianhydride (PTCDA), and 1,4,5,8-naphtalene-tetracarboxylic-dianhydride (NTCDA) (see their chemical structures in Fig. 1), were optimized using QChem[54] at the B3LYP/cc-pVTZ level. GKS eigenvalues were computed with QChem[54] using a cc-pVTZ basis set and the semilocal Perdew-Burke Ernzerhof (PBE) functional,[55] as well as the corresponding global hybrid, PBEh,[56, 57] and the LRC-hybrid LC-ωPBE[58] using the standard (ω=0.4 bohr^{-1}) and IP-

tuned range-separation parameters. The fractional particle curves for the evaluation of the MSIE were performed in a local development version of PSI4.[59]

The G_0W_0 calculations employed the all-electron numerical atom-centered orbital (NAO) code FHI-aims[21, 60, 61] and a *tier 4* basis set. In order to avoid issues with the starting point dependence of G_0W_0, which can be significant for the types of molecules studied in this work, the recently introduced consistent starting point (CSP) scheme was used.[22] For PTCDA and NTCDA, the CSP is 30% HF-exchange. In contrast to alternative semilocal DFT or HF starting points for G_0W_0, the CSP has been demonstrated to yield very accurate QP spectra for the molecules studied in this work. For 1,8-naphthalene-dicarboxylic anhydride (NDCA), a molecule similar to PTCDA and NTCDA, the mean absolute error (MAE) of G_0W_0@CSP with respect to PES is 0.1 eV, whereas the MAE of G_0W_0@PBE is 0.55 eV.[22] The improvement gained from using the CSP is particularly significant for sigma orbitals. For the highest occupied sigma orbital in NDCA, HOMO-2, the absolute error from comparison to experiment is reduced from 0.68 eV in G_0W_0@PBE to 0.1 eV in G_0W_0@CSP.[22]

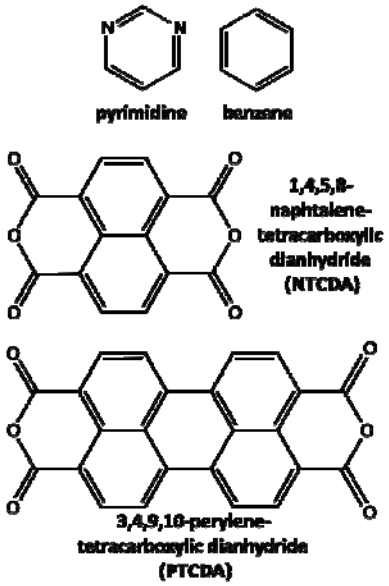

Figure 1: Molecules studied in this work.

4. Quasiparticle spectra from tuned LRC-hybrids

In the following, we assess the performance of tuned LRC-hybrids for PTCDA and NTCDA. The intricate electronic structure of these organic-semiconductor molecules has been the subject of several theoretical studies[8, 11-13, 22, 26, 27, 48] and it has been demonstrated that predicting their valence spectra correctly represents a major challenge for electronic-structure methods. At the same time, accurate experimental data for the ionization energies[62] and the nature of the corresponding orbitals[13, 14] exist, making PTCDA and NTCDA ideal test cases for the performance of tuned LRC hybrids in predicting QP spectra.

Figure 2 shows the comparison of the eigenvalue spectra obtained for PTCDA and NTCDA from PBEh and the standard and IP-tuned LC-ωPBE to the G_0W_0@CSP QP spectrum,[22] as well as the experimental PES.[62] Following common practice, the vibrational broadening is simulated by convolution of the eigenvalues with Gaussians and the HOMO eigenvalue and the experimental HOMO peaks are shifted to zero. We note that this alignment of the HOMO peaks in fact masks one of the main advantages of the tuned LRC hybrids, *i.e.*, their ability to predict very accurate IPs from the HOMO eigenvalue. This is a major difference to semilocal, global hybrid, and standard LRC hybrid functionals, for which the KS or GKS HOMO eigenvalues typically do not yield good approximations to the IP (see Table 1). However, since the superior performance of tuned LRC hybrids for IPs and fundamental gaps has already been well documented,[34, 38] we will not dwell on this question here. Rather, we are interested in the performance of tuned LRC hybrids for the *entire* valence spectrum. For this purpose, the alignment of HOMO peaks provides for a relevant, easy comparison of the various DFT functionals.

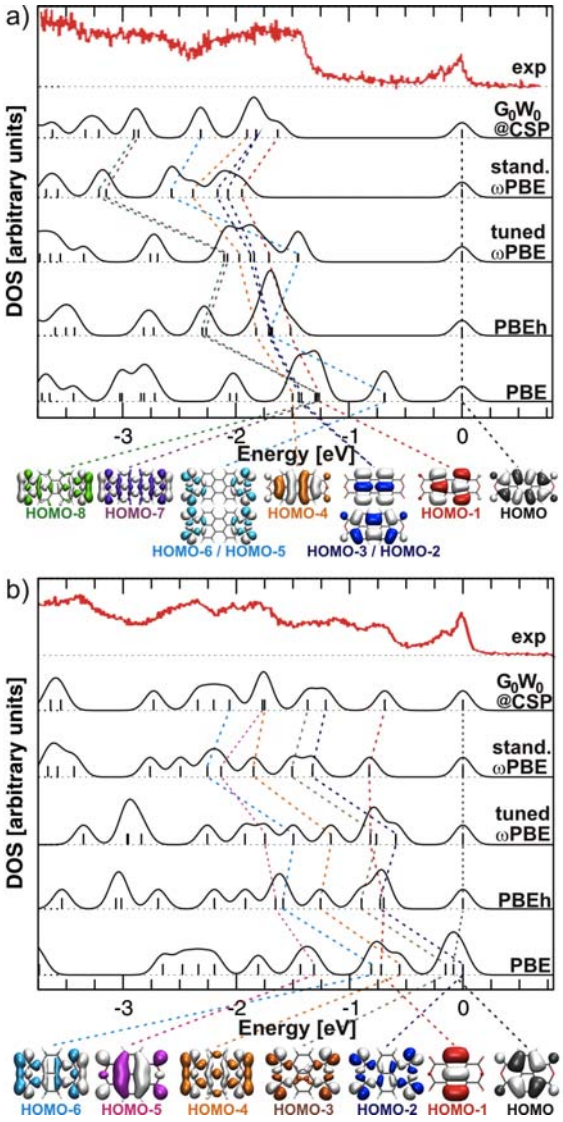

Figure 2: DOS for PTCDA (top) and NTCDA (bottom) from G_0W_0@CSP, standard LC-ωPBE, IP-tuned LC-ωPBE, and PBEh as compared to the experimental PES.[62]

	Exp.	G_0W_0@CSP	PBE		PBEh		LC-ωPBE		Tuned LC-ωPBE
			ΔSCF	ε_H	ΔSCF	ε_H	ΔSCF	ε_H	ΔSCF = ε_H
PTCDA	8.20	8.13	7.87	6.14	8.04	6.89	8.36	8.85	8.07
NTCDA	9.67	9.65	9.21	7.12	9.54	8.13	9.92	10.37	9.65

Table 1: HOMO eigenvalues and ΔSCF ionization energies from the different DFT approaches compared to G_0W_0@CSP energies and experimental gas phase IPs[62] for PTCDA and NTCDA in eV.

The frontier orbitals in PTCDA and NTCDA, shown in Fig. 2, generally fall into two categories: π orbitals delocalized over the perylene and naphthalene cores, respectively, and σ orbitals primarily located on the anhydride groups. Earlier analysis showed that the two types of orbitals suffer from significantly different OSIEs, leading to major spectral distortions in commonly used semilocal DFT approaches.[11, 12] Indeed, Fig. 2 confirms that predicting the correct relative position of the σ and π orbitals in PTCDA and NTCDA is a major challenge for approximate density functionals. Generally speaking, none of the employed DFT functionals satisfactorily matches the G_0W_0@CSP spectrum. Although the hybrid functionals clearly improve upon the semilocal PBE, they all show significant deviations from the G_0W_0@CSP benchmark, in particular in the positions of the σ orbitals located on the anhydride groups. For example, the global hybrid PBEh does not predict the correct orbital ordering for the σ and π orbitals in both PTCDA and NTCDA. This failure was demonstrated earlier for the B3LYP eigenvalue spectrum of PTCDA.[13]

Turning to the tuned LRC-hybrid, the comparison of the calculated eigenvalue spectra for PTCDA and NTCDA to the G_0W_0@CSP reference is even worse than in the case of the global and standard LRC hybrid functionals. As predicted by G_0W_0@CSP and confirmed by recent angular resolved photoelectron spectroscopy (ARPES) measurements on thin films,[13] the PES peak between -1.5 eV and -2.1 eV in the PTCDA spectrum has contributions from four π orbitals. Moreover, both the ARPES measurement and G_0W_0@CSP show the HOMO-2/HOMO-3 levels to be degenerate. The tuned LC-ωPBE, however, gives the second peak in the PTCDA spectrum to be a superposition of two σ-orbitals (HOMO-5/HOMO-6) and does not capture the degeneracy of the HOMO-2 and HOMO-3 eigenvalues. However, it has to be kept in mind that, due to the interactions with the substrate, the ordering of states obtained from ARPES measurements on a

thin film does not have to be necessarily exactly the same as in gas-phase experiments. Also, the ARPES signal intensity for σ orbitals is smaller than for π orbitals, which opens the possibility that the σ states might hardly be seen in ARPES. As a result, we have chosen to compare the QP energies related to σ orbitals to the most accurate theoretical benchmark data available for these systems, *i.e.*, G_0W_0@CSP energies.[22] From this comparison, it is clear that the tuned LC-ωPBE eigenvalue spectrum presents substantial errors, primarily for those eigenvalues that correspond to the σ orbitals located on the anhydride groups.

Of the functionals studied in Fig. 2, only standard LC-ωPBE captures the expected ordering of states. However, it also predicts too large level spacings and does not capture the degeneracy of the HOMO-2/HOMO-3 levels. In addition, standard LC-ωPBE does not predict accurate IPs and fundamental gaps (see Table 1). Based on the results shown in Figure 2, we conclude that tuning a LRC-hybrid functional to obtain highly accurate IPs does not guarantee the same level of accuracy for the entire valence spectrum. We now elaborate on the reason for that behavior.

In order to analyze the performance of the employed functionals in terms of the OMSIE, we considered the successive ionization of PTCDA and NTCDA up to the +10 cation in steps of 0.1 of an electron charge, using the standard and IP-tuned LC-ωPBE as well as the global hybrid PBEh. The deviation of the total energy curves from linearity, ΔE (see Eq. (3)), is provided in Figure 3. As expected, the global hybrid PBEh yields a significant delocalization error for all orbitals, which is as large as -0.20 eV for PTCDA and -0.26 eV for NTCDA. The standard LC-ωPBE leads to a localization error of around 0.1 eV for the π orbitals and a very small OMSIE (<0.01 eV) for the σ orbitals. The IP-tuned LC-ωPBE exhibits an opposite behavior with very small OMSIEs well below 0.01 eV for all π orbitals, but a significant delocalization error of

approximately 0.1 eV for the σ orbitals. The delocalization error in the σ orbitals is consistent with the too high energies of the corresponding eigenvalues. This imbalanced treatment of the σ and π orbitals helps rationalize the unsatisfactory performance of the IP-tuned LRC-hybrid for the prediction of the QP spectra of PTCDA and NTCDA.

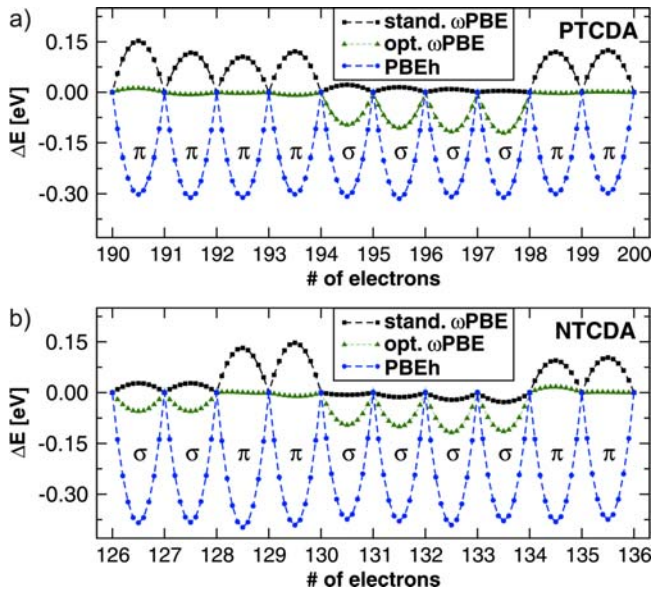

Figure 3: Many-electron self-interaction error for the ionization of PTCDA (top) and NTCDA (bottom) from standard LC-ωPBE (black squares), IP-tuned LC-ωPBE (green triangles), and PBEh (blue dots).

5. Global exchange vs. range-separation

In Ref. [48], it was demonstrated that the LRC-hybrid γBNL, in which the range-separation parameter γ is tuned by imposing Koopmans' condition on the anion, neutral, and cation states, shows the same drawbacks in terms of the QP spectra for PTCDA and NTCDA as the IP-tuned LC-ωPBE discussed in our work. Although the authors of Ref. 48 restricted their analysis of the OMSIEs to those of the HOMO and LUMO, both of which are π orbitals, they also suggested

that the problem was related to an imbalanced treatment of σ and π orbitals. Following earlier work by Srebro and Autschbach,[47] they proposed that the issue could be addressed by combining a fraction of short-range (SR) HF exchange with the LRC hybrid by partitioning the Coulomb operator according to:

$$\frac{1}{r} = \frac{\propto + (1-\propto) erf(\omega r)}{r} + \frac{(1-\propto)\,\mathrm{erfc}(\omega r)}{r} \qquad (6)$$

In the following, we refer to the functional resulting from replacing the Coulomb operator in LC-ωPBE by the one in Eq. (6) as LC-ωPBEα. This functional introduces the additional parameter α, *i.e.*, the amount of HF exchange employed in the SR part, and thus involves an additional (ideally non-empirical) constraint. In search for such a constraint on α, Refaely-Abramson *et al.* chose different values of α between 0 and 0.5, tuned the range-separation parameter by imposing Koopmans' condition on the anion, neutral, and cation states, and analyzed the MSIE in the HOMO eigenvalue when going from the dication to the anion. They showed that once the range-separation parameter was fixed, the σ orbitals located on the anhydride groups were sensitive to α, whereas the π orbitals delocalized over the perylene or naphthalene backbones were not. A value of α=0.2 was found to minimize the eigenvalue MSIE for the HOMO and LUMO orbitals of both PTCDA and NTCDA.[48] The authors concluded that the inclusion of SR HF exchange improves the agreement between the eigenvalue spectra obtained from tuned LRC-hybrids and their G_0W_0@PBE benchmark within the energy range studied in their work, *i.e.*, 3 eV below the IP. In the light of this finding and the results presented in Figure 3, we reexamine the performance of LC-ωPBE when including a fraction of HF exchange in the SR. In contrast to Ref. 48, our focus here lies on evaluating the OMSIE for both π and σ orbitals; thus, here, the

deeper eigenvalue spectrum is considered as well and we take two additional molecules into account, namely benzene and pyrimidine.

Following the method proposed by Refaely-Abramson *et al.*,[48] we varied α in LC-ωPBEα between 0 and 0.5 and tuned ω for each α separately using the IP-tuning procedure for PTCDA and NTCDA. For the case of PTCDA (top of Figure 4), we find ω values and eigenvalue spectra in very good agreement with Ref. [48], which underlines that the difference mentioned above in the tuning procedures does not have a significant influence on the obtained spectra.

Figure 4 shows the evolution of the GKS eigenvalues as a function of α for PTCDA and NTCDA. For PTCDA, the GKS eigenvalues corresponding to the π orbitals HOMO to HOMO-4 are not significantly affected by the variations in α. In contrast, the σ eigenvalues markedly change with α. The best agreement with the G_0W_0@CSP benchmark is found for α-values between 0.3 and 0.4, where the GKS eigenvalues approximate the theoretical benchmark within an error bar of 0.2 eV. Although the description of the eigenvalues corresponding to π orbitals is much better than for σ-type orbitals, it is not entirely without flaws. For example, the tuned LRC-hybrid does not capture the degeneracy of the HOMO-2 and HOMO-3 orbitals.

For NTCDA, the analysis is somewhat less conclusive with respect to the optimal value of α. In this case, it is not only the σ orbitals but also some of the π orbitals that show a significant dependence on α, as exemplified by HOMO-5, HOMO-7, and HOMO-8. In addition, there is no single α value for which all GKS eigenvalues match the G_0W_0 QP energies. When considering an error bar of 0.2 eV on the GKS eigenvalues, an approximate agreement with the G_0W_0@CSP energies is again found for α-values between 0.3 and 0.4.

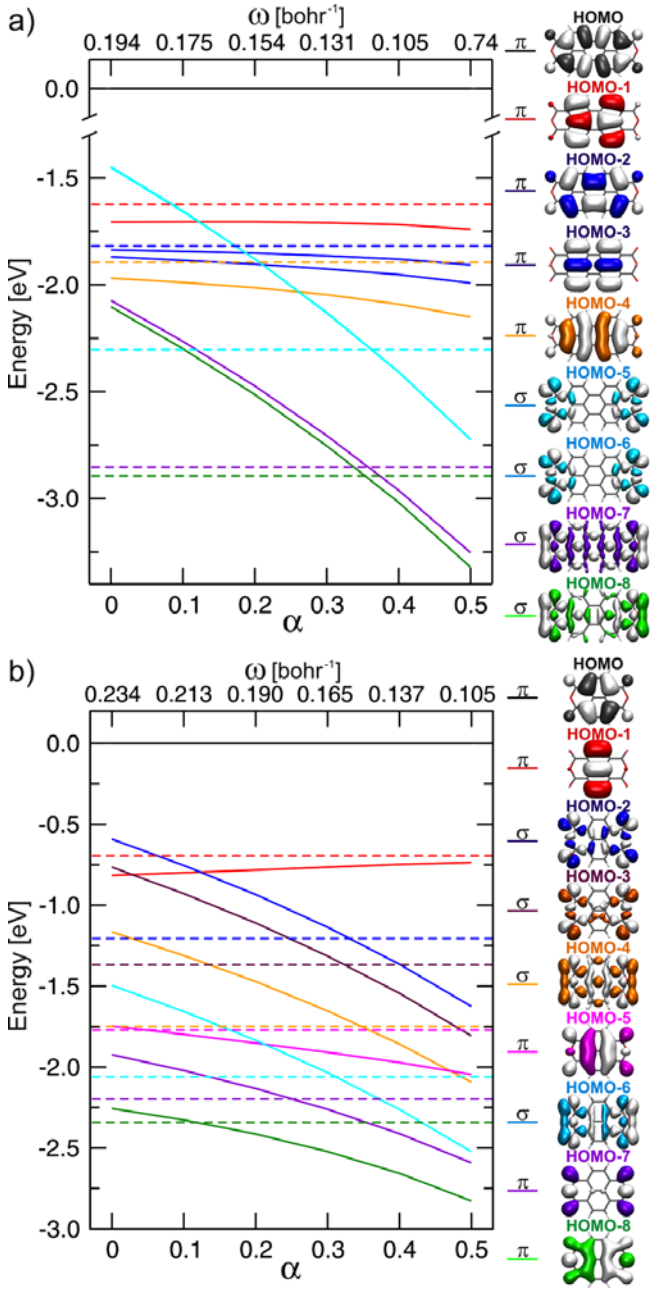

Figure 4: Highest occupied GKS eigenvalues (solid lines) as a function of fraction of HF exchange in the SR, α, for PTCDA (top) and NTCDA (bottom) computed from tuned LC-ωPBEα. G_0W_0@CSP energies are denoted as dashed horizontal lines. Eigenvalues for which the G_0W_0@CSP energies are degenerate are represented by the same color.

Figure 5 illustrates the analysis of the OMSIE for the ionization of the two highest occupied σ (left) and π (right) orbitals in PTCDA (top) and NTCDA (bottom). Several conclusions can be drawn from this figure. First, the OMSIE for the highest two occupied π orbitals is very small (well below 10^{-3} eV) and does not significantly depend on α. The differences among the OMSIEs for the different values of α are not significant (on the order of 10^{-4} eV) and no general trend in the evolution of the OMSIE with α can be found. This is not surprising since the IP-tuning procedure is known to significantly reduce the OMSIE for the HOMO and it was found earlier that similar types of orbitals display similar OMSIE values with LRC-hybrids.[51] In contrast, the highest two occupied σ orbitals show a significant delocalization error that decreases with increasing α. However, the OMSIE for the σ orbitals is not minimized in the range of α values studied here. In particular, a significant delocalization error is found in the range of α-values for which the best agreement of the GKS eigenvalues with the QP energies was found, *i.e.*, $0.3 < \alpha < 0.4$.

From the general trends illustrated in Figures 4 and 5, it is clear that, even if it were possible to find a combination of α and ω values for which the OMSIEs of both σ and π orbitals are minimized, this would not lead to a GKS eigenvalue spectrum that satisfactorily reproduces the G_0W_0 QP spectrum. Also, our results demonstrate that there is no single value of α for which the entire GKS valence spectrum matches the G_0W_0@CSP reference. It might still be possible to find tuning procedures for α and/or ω that improve the overall eigenvalue spectra obtained from the LRC-hybrids "on average". However, it is clear that while tuning the range-separation parameter to a single orbital with a particular character may yield a high level of accuracy for the IP, the same level of accuracy is not guaranteed for the entire valence spectrum.

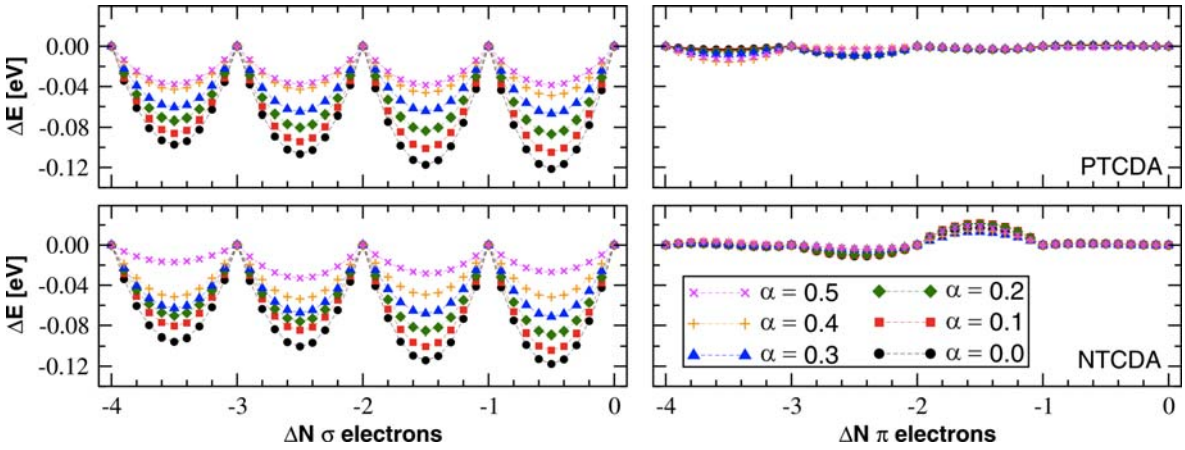

Figure 5: Deviation of the total energy from straight line, ΔE, for the ionization of the two highest occupied σ (left) and π (right) orbitals in PTCDA (top) and NTCDA (bottom) computed from LC-ωPBEα for different amounts of SR HF exchange, α, between 0 and 0.5.

At this stage, it would be interesting to find the source of the distinctly different behavior of π and σ orbitals of NTCDA and PTCDA and to understand the reason why only the σ (and not the π) orbitals of PTCDA seem to be affected by α. For this purpose, we have repeated the analysis of Figure 4 for the cases of benzene and pyrimidine (see Fig. 1), both of which have been studied extensively experimentally and theoretically (see Ref. [22] and references therein). While benzene and pyrimidine are very similar molecules in terms of their size and overall electronic structure, there is a major difference in the nature of their frontier orbitals: the HOMO of benzene is a (degenerate) π-orbital, while the HOMO of pyrimidine is a nonbonding orbital with dominant contributions from the nitrogen lone pairs. An important advantage of benzene and pyrimidine is that, in contrast to PTCDA and NTCDA, their PES shows distinct and separate peaks. Hence, we can directly compare to experimental ionization energies in addition to theoretical benchmark data. As the G_0W_0@CSP spectrum agrees well with the experimental PES, as confirmed by the small MAEs of 0.16 eV for benzene and 0.09 eV for pyrimidine, we only show the comparison to the experimental PES in the following.

Again, we employ LC-ωPBEα, obtain ω from IP-tuning, and vary α between 0 and 0.5. The evolution with α of the GKS eigenvalues obtained in this way is depicted in Figure 6. For benzene, the eigenvalues corresponding to the σ orbitals decrease by as much as 1 eV with α going from 0 to 0.5, while the π orbitals do not change significantly. As in the case of NTCDA and PTCDA, *α* has a negligible influence for those orbitals whose character is similar to that of the HOMO. For pyrimidine, the IP-tuning sets the eigenvalues corresponding to the *n*-type HOMO and all other orbitals of a similar nature, including HOMO-4 and HOMO-5, whereas the eigenvalues corresponding to the π orbitals strongly increase with α.

These results demonstrate that the different behavior of different types of orbitals with respect to α is a direct consequence of the tuning procedure. The IP-tuning does minimize the OMSIE for the HOMO and all orbitals of a similar character. The consequences are that: (i) the eigenvalues of the latter become essentially independent of the amount of HF exchange employed in the SR; and (ii) a change in α primarily influences eigenvalues that correspond to orbitals of a different character.

The comparison to experimental data shows that, similarly to NTCDA and PTCDA, there is no single α value such that the GKS eigenvalues match the reference data with adequate accuracy for the entire spectrum. Some GKS eigenvalues, such as the HOMO-4 in both benzene and pyrimidine, even deviate by more than 0.5 eV from the experimental ionization energies for the whole range of α values studied here. For pyrimidine, this also means a qualitative failure of LC-ωPBEα to reproduce the orbital ordering of HOMO-4 through HOMO-6.[63, 64]

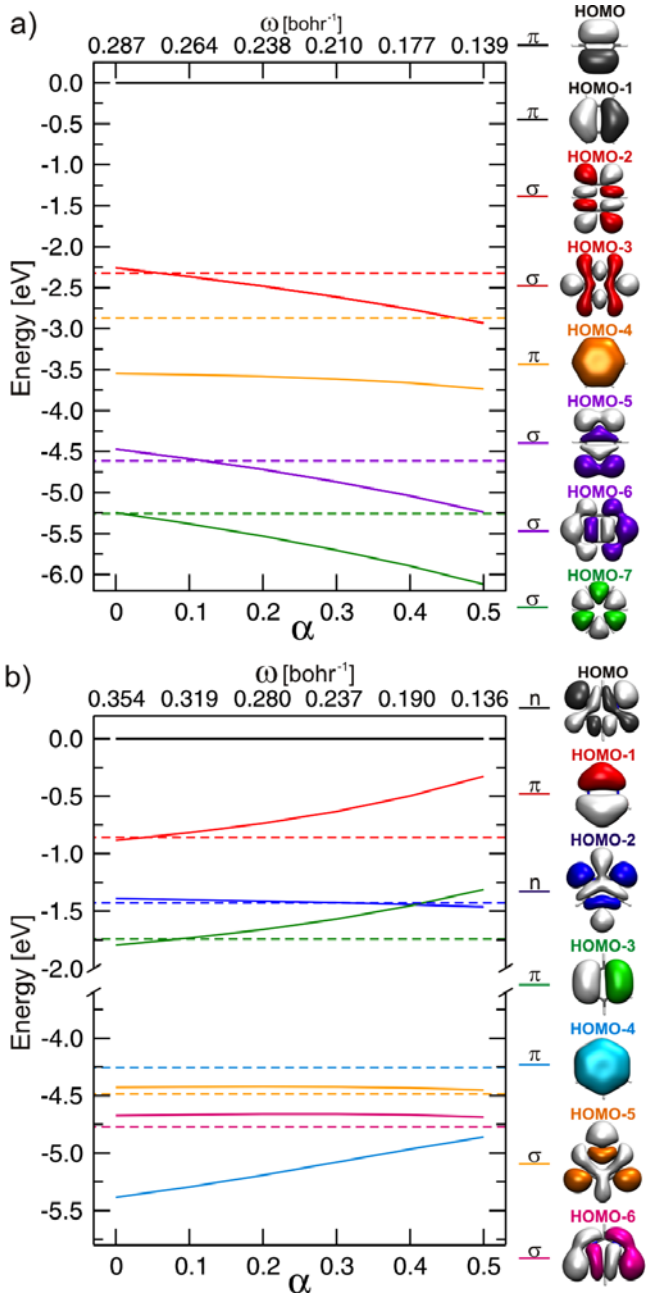

Figure 6: Highest occupied GKS eigenvalues (solid lines) as a function of fraction of HF exchange in the SR, α, for benzene (top) and pyrimidine (bottom), computed from LC-ωPBEα. Experimental ionization energies in gas-phase for benzene[65] and pyrimidine[66] are denoted as dashed horizontal lines. Eigenvalues for which the experimental (and G_0W_0@CSP) energies are degenerate are represented by the same color.

6. Conclusions

We have demonstrated, using representative molecules such as PTCDA, NTCDA, benzene, and pyrimidine, that the high level of accuracy obtained from tuned LRC-hybrid functionals for ionization potentials and fundamental gaps is not retained for the entire valence spectrum. This drawback can be rationalized by the observation that orbitals of different character, such as σ and π orbitals in conjugated molecules, require significantly different range-separation parameters to minimize their corresponding orbital-specific many-electron self-interaction errors. Thus, the IP-tuning of the range-separation parameter significantly reduces the OMSIE for the HOMO and all similar orbitals, but not for orbitals of a different nature.

To assess to what extent the inclusion of a suitable fraction of short-range HF exchange (α) can improve the accuracy of the GKS eigenvalue spectra, different non-empirical approaches to optimize α have been considered. No single value of α was found to provide a sufficiently accurate description of the entire QP spectrum as compared to the most accurate benchmark data available. Even if α is chosen empirically, such that the overall spectrum is as similar as possible to experiment and/or to benchmark calculations, the obtained GKS eigenvalues do not reach a level of accuracy comparable to G_0W_0 calculations that employ a reliable DFT starting point. We conclude that the existing schemes for the tuning of range-separated hybrid functionals have yet to achieve the accuracy of reliable *GW* methods for the calculation of quasi-particle spectra.

ACKNOWLEDGMENTS

We thank Peter Puschnig for stimulating discussions. The Center for Computational Molecular Science and Technology is funded through a NSF CRIF award (Grant No. CHE-0946869) and by the Georgia Institute of Technology. This work was partly supported by the AFOSR through the COMAS MURI program (agreement number FA9550-10-1-0558). TK thanks the AvH Foundation for financial support through the Feodor-Lynen program. RP thanks the U.S. Department of Energy for funding through the Computational Science Graduate Fellowship Program (DE-FG02-97ER25308). CDS acknowledges support from the US National Science Foundation (Grant No. CHE-1011360).

References

1. L. J. Sham and W. Kohn, Physical Review **145**, 561 (1966).
2. A. Seidl, A. Görling, P. Vogl, J. A. Majewski and M. Levy, Phys. Rev. B **53**, 3764 (1996).
3. N. Binggeli and J. R. Chelikowsky, Phys. Rev. Lett. **75**, 493 (1995).
4. I. G. Hill, A. Kahn, J. Cornil, D. A. dos Santos and J. L. Brédas, Chem. Phys. Lett. **317**, 444 (2000).
5. D. P. Chong, O. V. Gritsenko and E. J. Baerends, J. Chem. Phys. **116**, 1760 (2002).
6. V. Coropceanu, M. Malagoli, D. A. da Silva Filho, N. E. Gruhn, T. G. Bill and J. L. Brédas, Phys. Rev. Lett. **89**, 275503 (2002).
7. L. Kronik, R. Fromherz, E. Ko, G. Ganteför and J. R. Chelikowsky, Nature Materials **1**, 49 (2002).
8. N. Dori, M. Menon, L. Kilian, M. Sokolowski, L. Kronik and E. Umbach, Phys. Rev. B **73**, 195208 (2006).
9. N. Marom, O. Hod, G. E. Scuseria and L. Kronik, J. Chem. Phys. **128**, 164107 (2008).
10. N. Marom and L. Kronik, Appl. Phys. Mater. **95**, 159 (2009).
11. T. Körzdörfer, S. Kümmel, N. Marom and L. Kronik, Phys. Rev. B **79**, 201205(R) (2009).
12. T. Körzdörfer, S. Kümmel, N. Marom and L. Kronik, Phys. Rev. B **82**, 129903(E) (2010).
13. M. Dauth, T. Körzdörfer, S. Kümmel, J. Ziroff, M. Wiessner, A. Scholl, F. Reinert, M. Arita, and K. Shimada, Phys, Rev, Lett, **107**, 193002 (2011).
14. P. Puschnig, E. M. Reinisch, T. Ules, G. Koller, S. Soubatch, M. Ostler, L. Romaner, F. S. Tautz, C. Ambrosch-Draxl and M. G. Ramsey, Phys. Rev. B **84**, 235427 (2011).
15. L. Hedin, Physical Review **139**, A796 (1965).
16. M. S. Hybertsen and S. G. Louie, Phys. Rev. B **34**, 5390 (1986).
17. F. Caruso, P. Rinke, X. Ren, M. Scheffler and A. Rubio, Phys. Rev. B **86**, 081102 (2012).
18. N. Marom, J. E. Moussa, X. G. Ren, A. Tkatchenko and J. R. Chelikowsky, Phys. Rev. B **84**, 245115 (2011).
19. X. Blase, C. Attaccalite and V. Olevano, Phys. Rev. B **83**, 115103 (2011).
20. C. Faber, C. Attaccalite, V. Olevano, E. Runge and X. Blase, Phys. Rev. B **83**, 115123 (2011).
21. X. Ren, P. Rinke, V. Blum, J. Wieferink, A. Tkatchenko, A. Sanfilippo, K. Reuter and M. Scheffler, New Journal of Physics **14**, 053020 (2012).
22. T. Körzdörfer and N. Marom, Phys. Rev. B **86**, 041110(R) (2012).
23. J. F. Janak, Phys. Rev. B **18**, 7165 (1978).
24. J. P. Perdew, R. G. Parr, M. Levy and J. L. Balduz, Phys. Rev. Lett. **49**, 1691 (1982).
25. Y. Zhang and W. Yang, Theoretical Chemistry Accounts: Theory, Computation, and Modeling (Theoretica Chimica Acta) **103**, 346 (2000).
26. T. Körzdörfer, J. Chem. Phys. **134**, 094111 (2011).
27. T. Körzdörfer and S. Kümmel, Phys. Rev. B **82**, 155206 (2010).
28. In practice, these issues are often dealt with by applying a constant stretch to the valence spectrum and using a so called scissor operator to correct the gap [see e.g., N. Papageorgiou, Y. Ferro, E. Salomon, A. Allouche, J. M. Layet, L. Giovanelli, and G. Le Lay, Phys. Rev. B **68**, 235105 (2003); L. Segev, A. Salomon, A. Natan, D. Cahen, L. Kronik, F. Amy, C. K. Chan, and A. Kahn, Phys. Rev. B **74**, 165323 (2006); J. Hwang, E.-G. Kim, J. Liu, J.-L. Brédas, A. Duggal, and A. Kahn, The Journal of Physical Chemistry C **111**, 1378 (2006)]
29. V. Atalla, M. Yoon, F. Caruso, P. Rinke and M. Scheffler, to be published (2012).
30. M. Jain, J. R. Chelikowsky and S. G. Louie, Phys. Rev. Lett. 1**07**, 216806 (2011).

31. T. Stein, L. Kronik and R. Baer, J. Chem. Phys. 1**31**, 244119 (2009).
32. R. Baer, E. Livshits and U. Salzner, Annu. Rev. Phys. Chem. **61,** 85 (2010).
33. T. Körzdörfer, C. Sutton, J. S. Sears, and J. L. Brédas, J. Chem. Phys. **135,** 204107 (2011).
34. S. Refaely-Abramson, R. Baer and L. Kronik, Phys. Rev. B **84**, 075144 (2011).
35. A. Karolewski, T. Stein, R. Baer and S. Kummel, J. Chem. Phys. **134**, 151101 (2011).
36. N. Kuritz, T. Stein, R. Baer and L. Kronik, Journal of Chemical Theory and Computation 7, 2408 (2011).
37. J. S. Sears, T. Körzdörfer, C.-R. Zhang and J.-L. Brédas, J. Chem. Phys. **135**, 151103 (2011).
38. T. Stein, H. Eisenberg, L. Kronik, and R. Baer, Phys. Rev. Lett. **105**, 266802 (2010).
39. A. Savin and H.-J. Flad, International Journal of Quantum Chemistry **56**, 327 (1995).
40. J. D. Chai and M. Head-Gordon, J. Chem. Phys. **128** (8), 084106 (2008).
41. J. D. Chai and M. Head-Gordon, Phys. Chem. Chem. Phys. **10**, 6615 (2008).
42. T. M. Henderson, A. F. Izmaylov, G. E. Scuseria, and A. Savin, J. Chem. Phys. **127**, 221103 (2007).
43. T. M. Henderson, A. F. Izmaylov, G. E. Scuseria and A. Savin, Journal of Chemical Theory and Computation **4**, 1254 (2008).
44. T. M. Henderson, B. G. Janesko and G. E. Scuseria, J. Phys. Chem. A **112**, 12530 (2008).
45. A. V. Krukau, G. E. Scuseria, J. P. Perdew and A. Savin, J. Chem. Phys. 1**29**, 124103 (2008).
46. R. Haunschild and G. E. Scuseria, J. Chem. Phys. **132**, 224106 (2010).
47. M. Srebro and J. Autschbach, J. Phys. Chem. Lett. **3**, 576-581 (2012).
48. S. Refaely-Abramson, S. Sharifzadeh, N. Govind, J. B. Neaton, R. Baer and L. Kronik, Phys. Rev. Lett., in press, also arXiv: 1203.2357v3. (2012).
49. P. Mori-Sanchez, A. J. Cohen and W. Yang, J. Chem. Phys. **125**, 201102 (2006).
50. A. Ruzsinszky, J. P. Perdew, G. I. Csonka, O. A. Vydrov and G. E. Scuseria, J. Chem. Phys. **125**, 194112 (2006).
51. T. Körzdörfer, R. M. Parrish, J. S. Sears, C. D. Sherrill and J. L. Brédas, J. Chem. Phys. **137**, 124305 (2012).
52. P. Mori-Sanchez, A. J. Cohen and W. Yang, Phys. Rev. Lett. **100**, 146401 (2008).
53. T. Körzdörfer, in C*omplex Quantum Systems Seminar* (The University of Texas at Austin, Feb. 9th 2012).
54. Y. Shao, L. F. Molnar, Y. Jung, J. Kussmann, C. Ochsenfeld, S. T. Brown, A. T. B. Gilbert, L. V. Slipchenko, S. V. Levchenko, D. P. O'Neill, R. A. DiStasio, R. C. Lochan, T. Wang, G. J. O. Beran, N. A. Besley, J. M. Herbert, C. Y. Lin, T. Van Voorhis, S. H. Chien, A. Sodt, R. P. Steele, V. A. Rassolov, P. E. Maslen, P. P. Korambath, R. D. Adamson, B. Austin, J. Baker, E. F. C. Byrd, H. Dachsel, R. J. Doerksen, A. Dreuw, B. D. Dunietz, A. D. Dutoi, T. R. Furlani, S. R. Gwaltney, A. Heyden, S. Hirata, C. P. Hsu, G. Kedziora, R. Z. Khalliulin, P. Klunzinger, A. M. Lee, M. S. Lee, W. Liang, I. Lotan, N. Nair, B. Peters, E. I. Proynov, P. A. Pieniazek, Y. M. Rhee, J. Ritchie, E. Rosta, C. D. Sherrill, A. C. Simmonett, J. E. Subotnik, H. L. Woodcock, W. Zhang, A. T. Bell, A. K. Chakraborty, D. M. Chipman, F. J. Keil, A. Warshel, W. J. Hehre, H. F. Schaefer, J. Kong, A. I. Krylov, P. M. W. Gill and M. Head-Gordon, Physical Chemistry Chemical Physics **8**, 3172 (2006).
55. J. P. Perdew, K. Burke and M. Ernzerhof, Phys. Rev. Lett. **77**, 3865 (1996); Phys. Rev. Lett. **78**, 1396 (1997).
56. J. P. Perdew, M. Ernzerhof and K. Burke, J. Chem. Phys. **105**, 9982 (1996).
57. C. Adamo and V. Barone, J. Chem. Phys. **110**, 6158 (1999).
58. O. A. Vydrov and G. E. Scuseria, J. Chem. Phys. **125**, 234109 (2006).
59. J. M. Turney, A. C. Simmonett, R. M. Parrish, E. G. Hohenstein, F. A. Evangelista, J. T.

Fermann, B. J. Mintz, L. A. Burns, J. J. Wilke, M. L. Abrams, N. J. Russ, M. L. Leininger, C. L. Janssen, E. T. Seidl, W. D. Allen, H. F. Schaefer, R. A. King, E. F. Valeev, C. D. Sherrill and T. D. Crawford, Wiley Interdisciplinary Reviews: Computational Molecular Science **2**, 556 (2012).
60. V. Blum, R. Gehrke, F. Hanke, P. Havu, V. Havu, X. Ren, K. Reuter and M. Scheffler, Computer Physics Communications **180**, 2175 (2009).
61. V. Havu, V. Blum, P. Havu and M. Scheffler, Journal of Computational Physics **228**, 8367 (2009).
62. J. Sauther, J. Wusten, S. Lach and C. Ziegler, J. Chem. Phys. **131**, 034711 (2009).
63. R. Gleiter, V. Hornung and Heilbron.E, Helv. Chim. Acta **55**, 255 (1972).
64. N. Kishimoto and K. Ohno, Journal of Physical Chemistry A **104**, 6940 (2000).
65. S.-Y. Liu, K. Alnama, J. Matsumoto, K. Nishizawa, H. Kohguchi, Y.-P. Lee and T. Suzuki, J. Phys. Chem. A **115**, 2953 (2011).
66. N. Kishimoto and K. Ohno, J. Phys. Chem. A **104**, 6940 (2000).